

(NASA-CR-134672) EXPERIMENTAL
DETERMINATION OF TURBULENCE IN A GH₂-GOX
ROCKET COMBUSTION CHAMBER (Tulane Univ.)
46 p HC \$5.50
N74-33382
G3/33 Unclas 47926
CSCL 21B

EXPERIMENTAL DETERMINATION OF TURBULENCE
IN A GH₂ - GOX ROCKET COMBUSTION CHAMBER

by

P. Tou, R. Russell, J. O'Hara

TULANE UNIVERSITY

prepared for



NATIONAL AERONAUTICS AND SPACE ADMINISTRATION

NASA Lewis Research Center
Grant NGR-19-002-030
Richard J. Priem, Project Manager

NOTICE

This report was prepared as an account of Government-sponsored work. Neither the United States, nor the National Aeronautics and Space Administration (NASA), nor any person acting on behalf of NASA:

- A.) Makes any warranty or representation, expressed or implied, with respect to the accuracy, completeness, or usefulness of the information contained in this report, or that the use of any information, apparatus, method, or process disclosed in this report may not infringe privately-owned right; or
- B.) Assumes any liabilities with respect to the use of, or for damages resulting from the use of, any information, apparatus, method or process disclosed in this report.

As used above, "person acting on behalf of NASA" includes any employee or contractor of NASA, or employee of such contractor, to the extent that such employee or contractor of NASA or employee of such contractor prepares, disseminates, or provides access to any information pursuant to his employment or contract with NASA, or his employment with such contractor.

Requests for copies of this report should be referred to

National Aeronautics and Space Administration
Scientific and Technical Information Facility
P. O. Box 33
College Park, Md. 20740

1. Report No. NASA CR-134672		2. Government Accession No.		3. Recipient's Catalog No.	
4. Title and Subtitle Experimental Determination of Turbulence in a CH ₂ -GOX Rocket Combustion Chamber				5. Report Date August 1974	
				6. Performing Organization Code	
7. Author(s) P. Tou, R. Russell and J. O'Hara				8. Performing Organization Report No.	
9. Performing Organization Name and Address Tulane University New Orleans, Louisiana 70118				10. Work Unit No.	
				11. Contract or Grant No. NGR 19-002-030	
12. Sponsoring Agency Name and Address National Aeronautics and Space Administration Washington, D.C. 20546				13. Type of Report and Period Covered	
				14. Sponsoring Agency Code	
15. Supplementary Notes Project Manager, Richard J. Priem, Chemical Propulsion Division, NASA Lewis Research Center, Cleveland, Ohio					
16. Abstract The intensity of turbulence and the Lagrangian correlation coefficient for a gaseous rocket combustion chamber have been determined from the experimental measurements of the tracer gas diffusion. A combination of Taylor's turbulent diffusion theory and Spalding's numerical method for solving the conservation equations of fluid mechanics was used to calculate these quantities. Taylor's theory was extended to consider the inhomogeneity of the turbulence field in the axial direction of the combustion chamber. An exponential function was used to represent the Lagrangian correlation coefficient. The results indicate that the maximum value of the intensity of turbulence is about 15% and the Lagrangian correlation coefficient drops to about 0.12 in one inch of the chamber length.					
17. Key Words (Suggested by Author(s)) Gas rockets Combustion Turbulence			18. Distribution Statement Unclassified-unlimited		
19. Security Classif. (of this report) Unclassified		20. Security Classif. (of this page) Unclassified		21. No. of Pages 44	
				22. Price* \$3.00	

FORWARD

The research reported herein was performed by the Mechanical Engineering Department of Tulane University under NASA Grant NGR 19-002-030 from January 1972 through December 1973. The project manager was Dr. Richard J. Priem, Chemical Rockets Division, NASA Lewis Research Center.

ABSTRACT

The intensity of turbulence and the Lagrangian correlation coefficient for a gaseous rocket combustion chamber have been determined from the experimental measurements of the tracer gas diffusion. A combination of Taylor's turbulent diffusion theory and Spalding's numerical method for solving the conservation equations of fluid mechanics was used to calculate these quantities. Taylor's theory was extended to consider the inhomogeneity of the turbulence field in the axial direction of the combustion chamber. An exponential function was used to represent the Lagrangian correlation coefficient.

The results indicate that the maximum value of the intensity of turbulence is about 15% and the Lagrangian correlation coefficient drops to about 0.12 in one inch of the chamber length.

TABLE OF CONTENTS

Symbols	vi
Summary	1
I. Introduction	2
II. Experiment	4
(1) Rocket Engine	4
(2) Experiment Procedure	4
(3) Analysis of Sample	7
(4) Experimental Data	8
III. Analysis of the Experimental Results	14
(1) Equations of the Turbulent Diffusion	14
(2) Analytical Determination of the Mean Axial Flow Velocity	15
(3) Determination of the Turbulent Parameters	19
IV. Analytical Determination of the Helium Concentration	27
(1) Preliminary Remarks	27
(2) Governing Equations	27
(3) Boundary Conditions	28
(4) Calculation Procedure and Results	30
V. Conclusions	36
References	37

LIST OF FIGURES

Figure		Page
1	Experimental Configuration	5
2	Experimental Helium Concentration Data	9
3	Experimental Mean Square Dispersion Radius	12
4	Mean Axial Flow Velocity	18
5	Comparison of Experimental and Calculated Mean Square Dispersion Radii	22
6	Root Mean Square Turbulent Velocity	25
7	The Intensity of Turbulence	26
8	The Boundary Conditions for Determining the Helium Concentration	29
9	Comparison of Calculated and Experimental Helium Concentration Profiles	32

SYMBOLS

Latin Characters

A_I	Cross-sectional area of the helium injector opening
a	Coefficient in the standard differential equation
b	Coefficient in the standard differential equation
c	Coefficient in the standard differential equation
D_j	Diffusion coefficient of species j
d	Coefficient in the standard differential equation; also combustion chamber diameter
f	Mixture fraction
k	Constant in the effective viscosity formula
l	Combustion chamber length
m_j	Concentration of species j
\dot{m}_j	Mass flow rate of species j
p	Static pressure
R_L	Lagrangian correlation coefficient
r	Coordinate
$\overline{r^2}$	Mean square dispersion radius
Sc	Schmidt number
T	The intensity of turbulence
t	Diffusion time
u	Velocity in the axial direction
v	Velocity; also velocity in the radial direction
x	Coordinate
y	Coordinate
z	Coordinate

Greek Characters

α	Constant in the expression for the Lagrangian correlation coefficient
θ	Circumferential angle
μ	Viscosity
ρ	Density
τ	Difference in diffusion times
ϕ	A dependent variable
ψ	Stream function
ω	Vorticity

Indices

eff	Effective value
He	Helium
I	Helium injection location
j	Species j
S	Sampling station
'	Fluctuating quantity
-	Mean quantity

SUMMARY

The intensity of turbulence and the Lagrangian correlation coefficient in a gaseous rocket combustion chamber have been determined experimentally using a small rocket engine operated at a nominal chamber pressure of 150 psia. The experimental method consisted of injecting a tracer gas at a point along the chamber centerline while taking samples along a diameter at a downstream station. Three sampling stations were investigated. Several injection points were used for each of the sampling stations.

The gas samples were analyzed using a combination of weighing, Orsat analyzer and gas chromatography to determine the tracer gas concentration profiles. The turbulent parameters were then calculated from the tracer gas concentration data using a combination of G.I. Taylor's turbulent diffusion theory and D.B. Spalding's numerical procedure for solving the conservation equations of fluid mechanics. Taylor's theory was extended to consider the inhomogeneity of the turbulence field in the axial direction of the combustion chamber. The Lagrangian correlation coefficient was represented by an exponential function of the form $e^{-\alpha\tau}$ where τ is the difference of the dispersion times of a fluid particle and α is a constant.

The results indicate that the values of the intensity of turbulence vary from a maximum of approximately 15% near the injector to 4% at the nozzle entrance. The Lagrangian correlation coefficient drops to 0.12 in one inch of the chamber length.

I. INTRODUCTION

Turbulent mixing is one of the most important physical processes occurring in a gaseous rocket combustion chamber. It influences the combustion process and therefore the performance of the rocket engine. In the theory of turbulent flow, the turbulent mixing of gases is quantitatively expressed in terms of the intensity of turbulence and the Lagrangian correlation coefficient. At present there are very little data available regarding these quantities, and only two previous attempts have been made to experimentally measure the intensity of turbulence under the actual conditions of a rocket combustion chamber.

Hersch⁽¹⁾ experimentally determined the intensity of turbulence in a two-dimensional hydrogen-liquid oxygen rocket combustion chamber from the measurements of the diffusion of a photographically visible tracer material. Hersch made the assumption that the turbulence field was homogeneous and the Lagrangian correlation coefficient was unity. The intensity of turbulence was calculated from the tracer diffusion data using the equations developed by Bittker⁽²⁾.

O'Hara et al.⁽³⁾ investigated the intensity of turbulence in a cylindrical liquid oxygen-heptane rocket engine. Their method consisted of experimentally measuring the diffusion of the helium tracer gas. The intensity of turbulence and the Lagrangian correlation coefficient were calculated from the diffusion measurements using a combination of Taylor's⁽⁴⁾ turbulent diffusion theory and the Fick diffusion equation. In the analysis, the turbulence field was assumed

to be isotropic throughout the combustion chamber and homogeneous only in the radial and circumferential directions, but not in the axial direction. The Lagrangian correlation coefficient was assumed to be an exponential function of the dispersion time.

The objective of the present work is to investigate the intensity of turbulence and the Lagrangian correlation coefficient in a gaseous oxygen (GOX)-gaseous hydrogen (GH₂) rocket combustion chamber. These quantities were experimentally determined from tracer gas diffusion measurements similar to that used by O'Hara et al. A combination of Taylor's turbulent diffusion theory and Spalding's⁽⁵⁾ numerical procedure for solving the conservation equations of fluid mechanics was used to calculate the intensity of turbulence and the Lagrangian correlation coefficient.

II. EXPERIMENT

(1) Rocket Engine

A small rocket engine using gaseous oxygen and gaseous hydrogen operating at a nominal chamber pressure of 150 psia was used in the experiment (see Figure 1). The propellents were injected in the form of co-axial jets from seven ports on the injector. Helium was used as the tracer gas and could be injected at various points along the center line of the combustion chamber. A probe passing across the chamber along a diameter was used to withdraw gas samples. This probe containing six sample ports could be moved laterally across the chamber or rotated circumferentially about the chamber centerline. Further, the sample probe could be placed at several longitudinal stations.

(2) Experimental Procedure

An automatic timing device was used to fire the rocket engine and take samples. About 1 1/2 seconds were required for the engine to reach equilibrium. During this time the sample lines were vented to the atmosphere. The helium tracer gas was injected during start-up so that it would also reach an equilibrium condition. Samples were withdrawn for about one second. The samples were collected in sample bottles for later analysis.

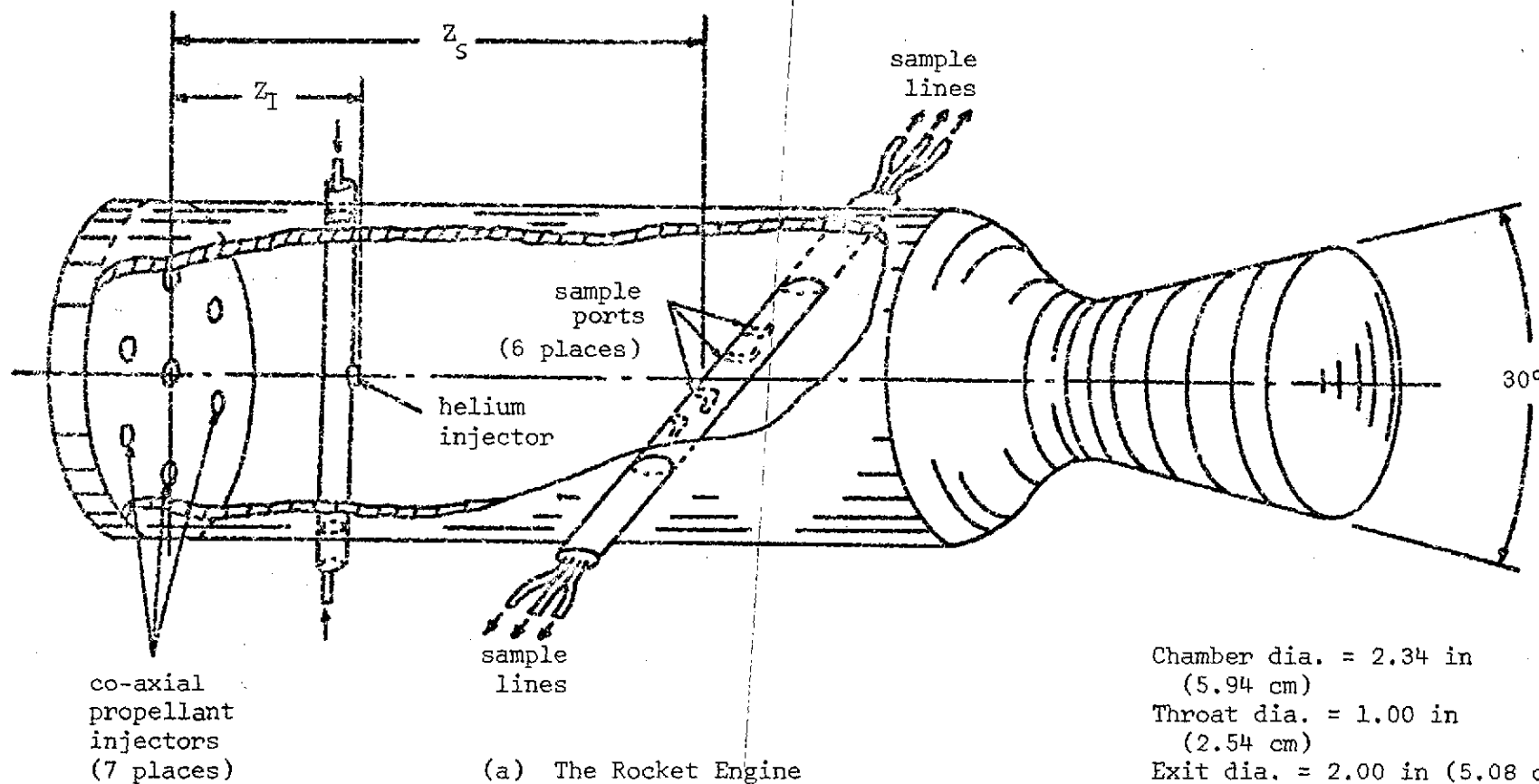
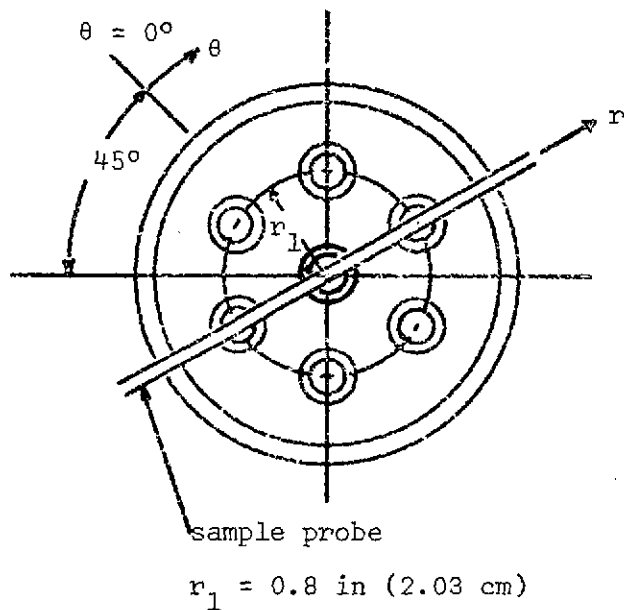


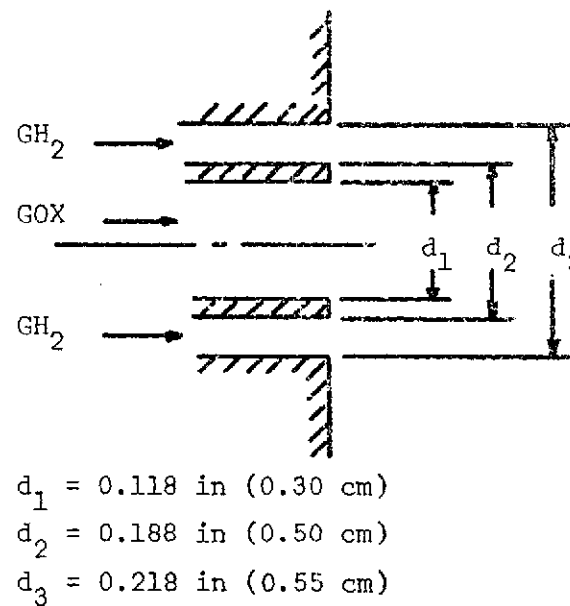
Figure 1
Experimental Configuration

Chamber dia. = 2.34 in
(5.94 cm)
Throat dia. = 1.00 in
(2.54 cm)
Exit dia. = 2.00 in (5.08 cm)
Mass flow rate GOX = .47 lb/sec
(.21 Kg/sec)
Mass flow rate GH_2 = .086 lb/sec
(.038 Kg/sec)

(b) Propellant Injector Plate



(c) Typical Propellant Injector



Sample Probe Positions:

- $\theta = 105^\circ$ - Sample on outer injectors
- $\theta = 135^\circ$ - Sample between outer injectors

Figure 1 Experimental Configuration
(Continued)

REPRODUCTION OF THE
ORIGINAL PAGE IS POOR

(3) Analysis of Sample

A method combining weighing, absorption and gas chromatography was used to analyze each sample containing water (H_2O), oxygen (O_2), hydrogen (H_2) and helium (He).

More than 90% by weight of the sample was water which could not be determined either by absorption or by gas chromatography. Therefore the sample bottle was weighed before the analysis, and again after the analysis was completed and the sample bottle was evacuated by a vacuum pump, so that the total weight of the sample could be determined.

Before the analysis was to begin, the sample bottle was charged with argon (Ar) to a pressure of 20 psig at the room temperature. With the pressure and temperature of the sample known, the weights of its components could be easily determined later from the results of the analysis.

The amount of oxygen and most of the hydrogen were measured by selective absorption using an Orsat analyzer. The absorption method was used because it was well suited for analyzing these gases in large concentrations. Also, oxygen and hydrogen tend to contaminate the chromatographic column.

The remaining sample which contained argon, helium and a small amount of hydrogen was analyzed using gas chromatography to determine the concentration of helium and hydrogen in a manner similar to that given by Villalobos and Nuss⁽⁶⁾. A Linde 5A molecular sieve column was used with argon as the carrier gas.

(4) Experimental Data

Gas samples were taken from three longitudinal stations along the combustion chamber. For each of these stations a series of helium injection points along the chamber centerline were investigated. Further, two circumferential angles of the sample probe with respect to the outer propellant injectors were used.

Three of the many helium concentration profiles are shown in Figure 2. The experimental data are scattered. The scattering is believed due to an instability of the flow in the combustion chamber. Many researchers⁽⁷⁾ of turbulence have shown that the distribution of the helium concentration downstream from a point source in a turbulent flow is Gaussian. Therefore the experimental data were assumed to obey the Gaussian distribution:

$$m_{\text{He}} = m_{\text{He},0} e^{-r^2 / 2 \overline{r^2}} \quad (1)$$

where $m_{\text{He},0}$ is the helium concentration at $r = 0$, and $\overline{r^2}$ is the mean square dispersion radius. The method of least squares was used to obtain the best fit of the experimental data to Equation 1. The curves in Figure 2 show the results of the curve fitting.

It is noted in Figures 2[a] and 2[b] that the values of $\overline{r^2}$ compare closely with each other. This shows that the helium concentration does not vary significantly with the circumferential angles of the sample probe and the assumption of the circumferential homogeneity of turbulence in the combustion chamber is satisfactory.

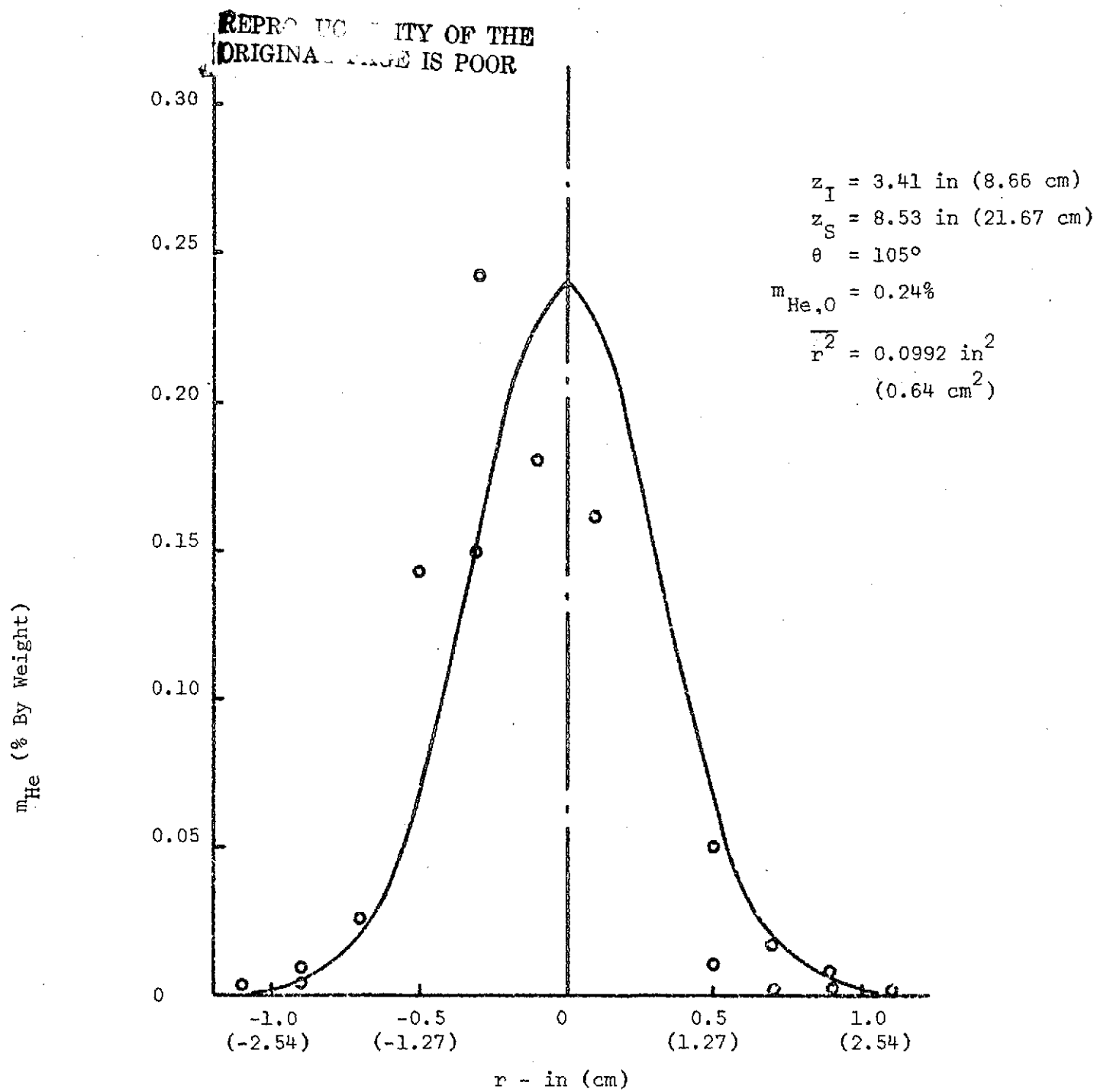


Figure 2a, Experimental Helium
Concentration Data

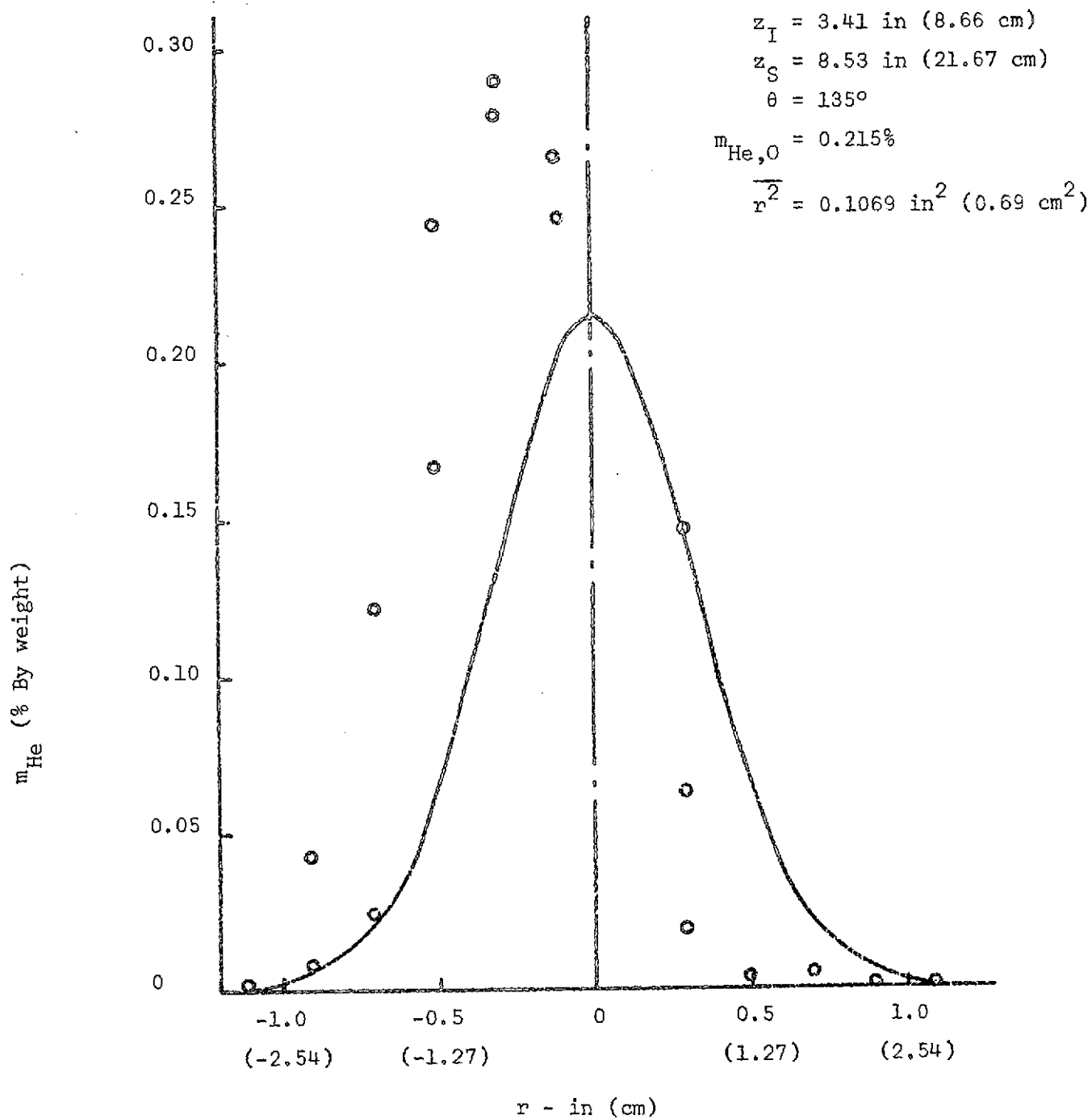


Figure 2b, Experimental Helium Concentration Data

REPRODUCIBILITY OF THE
ORIGINAL PAGE IS POOR

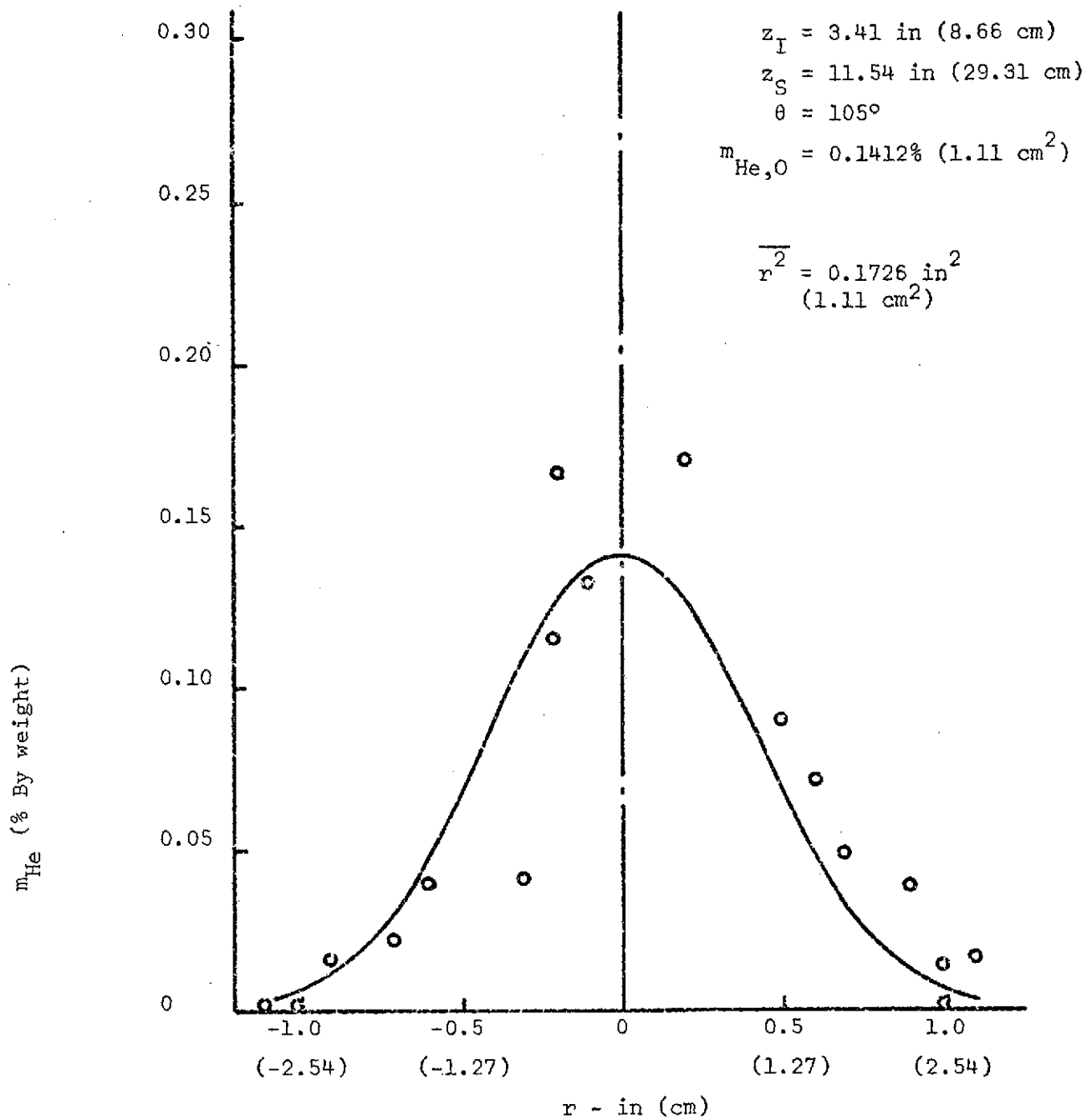
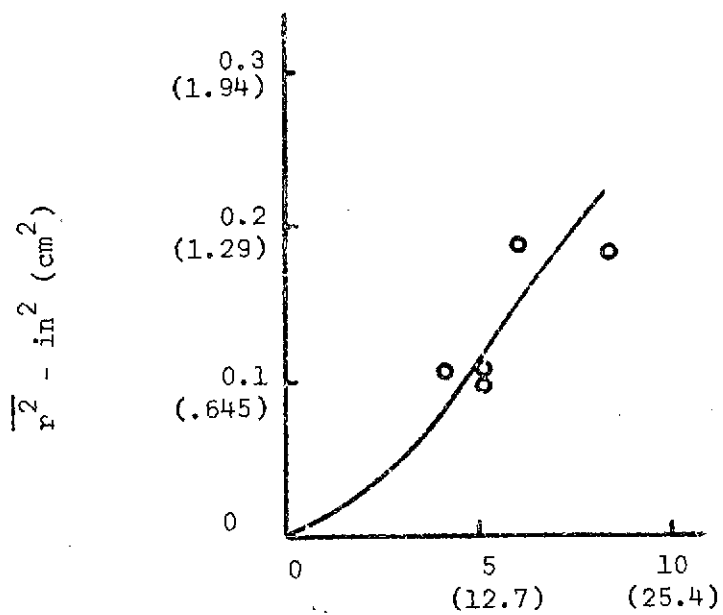
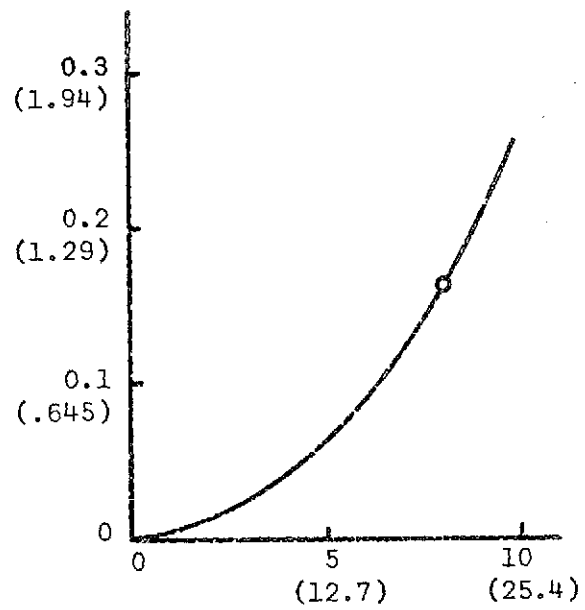


Figure 2c, Experimental Helium
Concentration Data



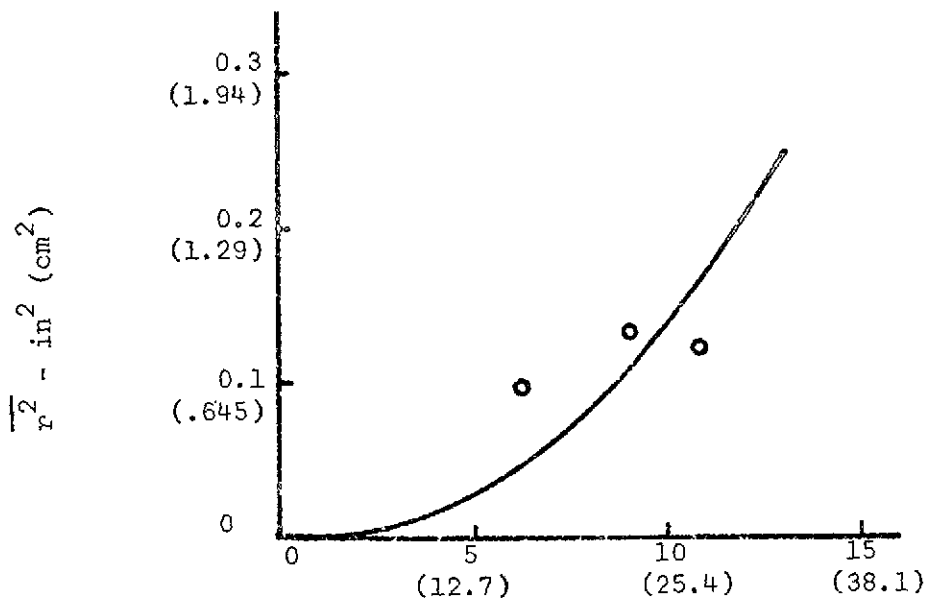
$z_S - z_I - \text{in (cm)}$

(a) $z_S = 8.53 \text{ in (21.67 cm)}$



$z_S - z_I - \text{in (cm)}$

(b) $z_S = 11.54 \text{ in (29.31 cm)}$



$z_S - z_I - \text{in (cm)}$

(c) $z_S = 14.3 \text{ in (36.32 cm)}$

Figure 3 Experimental Mean Square Dispersion Radius

The values of $\overline{r^2}$ as a function of the distance between the helium injection point and the sampling station are plotted in Figure 3 for the three sampling stations investigated. These results were used to determine the intensity of turbulence and Lagrangian correlation coefficient.

III. ANALYSIS OF THE EXPERIMENTAL RESULTS

(1) Equations of the Turbulent Diffusion

In analyzing the turbulent diffusion in a flow field, G.I. Taylor used the Lagrangian approach by considering the path of a marked fluid particle during its motion through the flow field, and developed an equation relating the displacement of the particle to the turbulent velocity. This formulation was based on the assumption that the turbulence was isotropic and homogeneous throughout the flow field.

For the present work, Taylor's turbulent diffusion theory was employed to analyze the turbulent diffusion in the combustion chamber. However, the original assumption was extended to consider that the turbulence field was inhomogeneous in the axial direction. Based on this assumption, the equation for the mean square dispersion radius, $\overline{r^2}$, in the cylindrical coordinates can be written as

$$\overline{r^2} = 4 \int_0^t dt' \int_0^{t'} R_L(\tau) \sqrt{\overline{v'^2}(t')} \sqrt{\overline{v'^2}(t'')} dt'' \quad (2)$$

where t' and t'' are two dispersion times of the same fluid particle and $\tau = t'' - t'$.

The Lagrangian correlation coefficient, $R_L(\tau)$, in Equation 2 is defined as

$$R_L(\tau) = \frac{\overline{v'(t')v'(t'')}}{\sqrt{\overline{v'^2}(t')} \sqrt{\overline{v'^2}(t'')}} \quad (3)$$

In order to solve Equation 2, it is necessary that the Lagrangian

correlation coefficient should be represented by a suitable function. Measurements of turbulent flows by many researchers⁽⁷⁾ have shown that the Lagrangian correlation coefficient can be roughly represented by an exponential function. In particular, Taylor also used an exponential function in his formulation. For the present work, the Lagrangian correlation coefficient was approximated by the form:

$$R_L(\tau) = e^{-\alpha\tau} \quad (4)$$

where α is a constant.

The variables $\overline{r^2}$, R_L , and $\sqrt{\frac{v'^2}{2}}$ in Equation 2 are functions of the dispersion time. Since the flow in the combustion chamber is considered to be steady, the dispersion time t required for a fluid particle to travel an axial distance from the point of release, z_I , to any point of interest, z , is related to the axial coordinate by the expression:

$$t = \int_{z_I}^z \frac{dz}{\overline{u}(z)} \quad (5)$$

where \overline{u} is the mean axial flow velocity. Therefore these variables are also a function of z .

The mean axial flow velocity was not measured in the experiment, but was determined by an analytical method.

(2) Analytical Determination of the Mean Axial Flow Velocity

Since there are seven co-axial propellant injection elements in the combustion chamber, the flow field is three-dimensional. Mathematically it would be very difficult to solve such a three-dimensional problem. To simplify the problem, the turbulent mixing of one chemically reacting,

co-axial jet is considered. This co-axial jet is assumed to be surrounded by an imaginary, cylindrical enclosure whose cross-sectional area is 1/7 of that of the actual combustion chamber. Thus the problem becomes an axisymmetric one.

To solve this problem the numerical procedure for solving the conservation equations developed by D.B. Spalding et al.⁽⁵⁾ was used. The uniqueness of Spalding's approach lies in the transformation of the conservation equations into a standard form which is a nonlinear partial differential equation of the elliptic type. This standard equation is then solved by a finite difference procedure, using the Gauss-Seidel iterative technique.

As presented in Reference 5, the standard equation in the cylindrical coordinates takes the form

$$\begin{aligned} a \left\{ \frac{\partial}{\partial z} \left(\phi \frac{\partial \psi}{\partial r} \right) - \frac{\partial}{\partial r} \left(\phi \frac{\partial \psi}{\partial z} \right) \right\} - \frac{\partial}{\partial z} \left\{ b \frac{\partial}{\partial z} (c\phi) \right\} \\ - \frac{\partial}{\partial r} \left\{ b \frac{\partial}{\partial r} (c\phi) \right\} + d = 0 \end{aligned} \quad (7)$$

where ϕ is the particular dependent variable, and a , b , c and d are coefficients which depend on geometric variables, material properties and other dependent variables.

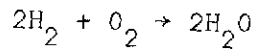
The important considerations inherent to the computational results are the modeling of turbulent viscosity and combustion. For the flow in a cylindrical chamber, spalding suggests that the effective viscosity,

μ_{eff} , may be expressed in the form

$$\mu_{eff} = k \cdot d^{2/3} l^{-1/3} \rho^{2/3} (\dot{m}_F v_F^2 + \dot{m}_O v_O^2)^{1/3} \quad (8)$$

A value of k equal to 0.012 was found suitable for the present work. The validity of this viscosity model was checked by comparing the experimental and calculated tracer gas concentration data. A method for calculating the tracer gas concentration will be discussed later.

In modeling the combustion, the combustion process is assumed to follow the simple chemical reaction



The reaction rate is assumed to be infinite, i.e., as soon as fuel and oxidizer come into contact, they react instantaneously at the stoichiometric mixture ratio.

The numerical solution of the governing equations for predicting the flow field of the single co-axial jet in the imaginary enclosure was obtained in terms of the vorticity ω , a stream function ψ , and the mixture fraction f . A computer program for calculating these variables is presented in Reference 5. From the mixture fraction the distribution of the density ρ was computed. The mean axial flow velocity was obtained from the definition of the stream function by using the approximation

$$\bar{u} = \frac{1}{P_{ave} r} \frac{\Delta\psi}{\Delta r} \quad (9)$$

where P_{ave} is the arithmetic average of the density across the radius of the enclosure at an axial position, $\Delta\psi$ is the difference between the value of the stream function at the enclosure and that at the axis of symmetry, and Δr is equal to the radius of the enclosure.

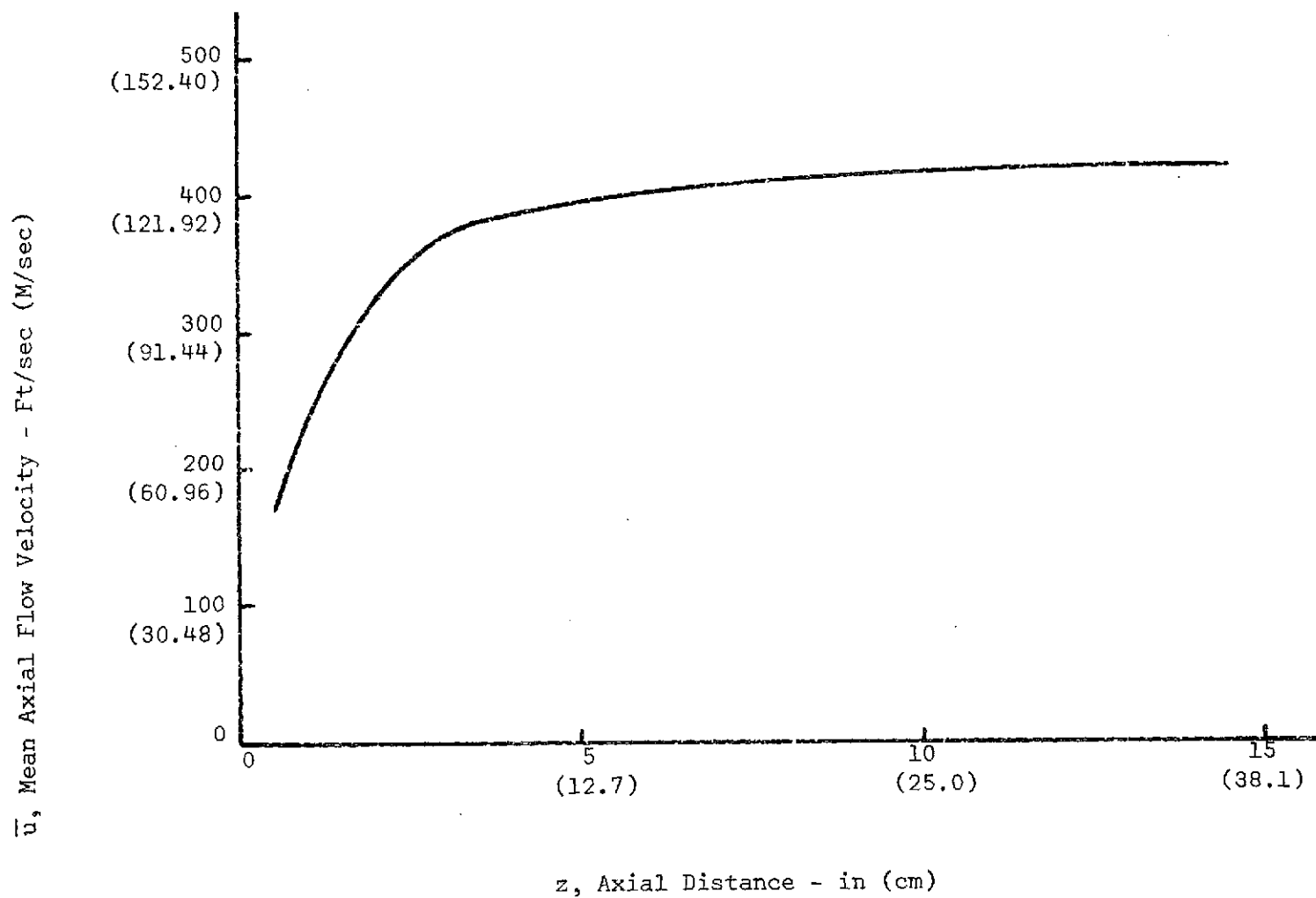


Figure 4, Mean Axial Flow Velocity

The mean axial flow velocity as a function of the axial chamber distance is plotted in Figure 4.

(3) Determination of the Turbulent Parameters

From the experimental results of the mean square dispersion radii, Equation 2 can now be solved for the root mean square (rms) turbulent velocity using a numerical method. The calculation procedure is as the following.

With the mean square dispersion radius as a known variable and assuming a value for α in the expression for the Lagrangian correlation coefficient, a first approximation of the rms turbulent velocity as a function of the z coordinate was calculated from Equation 2. Then the calculation procedure for the equation was reversed. Considering the rms turbulent velocity as a known variable and using the same value for α as before, the equation was solved for $\overline{r^2}$. The calculated and experimental values of $\overline{r^2}$ were compared. This calculation procedure was repeated by adjusting the values of the rms turbulent velocity until a best possible agreement between the calculated and experimental values of $\overline{r^2}$ was achieved.

The above calculations were repeated for a range of values for α ($\alpha = 100 \text{ sec}^{-1}$, 4000 sec^{-1} , 10000 sec^{-1} and 20000 sec^{-1}).

The comparison of the calculated and experimental values of $\overline{r^2}$ is shown in Figure 5. The resulting rms turbulent velocities for different values of α are shown in Figure 6.

From the results shown in Figure 5, it can be seen that the curves for $\alpha = 10000 \text{ sec}^{-1}$ appear to give the best fit for the experimental data, and the curves for $\alpha = 100 \text{ sec}^{-1}$ do not appear to fit the experimental data. Therefore, $\alpha = 10,000 \text{ sec}^{-1}$ is the best choice for the constant in the exponential expression for the Lagrangian correlation coefficient. The rms turbulent velocity for the combustion chamber is represented in Figure 6 by the curve with $\alpha = 10000 \text{ sec}^{-1}$.

Although $\alpha = 10000 \text{ sec}^{-1}$ is the best choice for the constant in the exponential expression for the Lagrangian correlation coefficient, the curves in Figure 5 show that good agreement between the calculated and experimental values of $\overline{r^2}$ also exists for large values of α , namely $\alpha = 4000 \text{ sec}^{-1}$ and $\alpha = 20000 \text{ sec}^{-1}$. Consequently the rms turbulent velocities with $\alpha = 4000 \text{ sec}^{-1}$ and $\alpha = 20000 \text{ sec}^{-1}$ shown in Figure 6 may also be those for the combustion chamber. In other words, the choice of the rms turbulent velocity depends upon the choice of the value for α , as long as α is large. This can be explained by approximating the integration in Equation 2.

With a change of the integration variable, Equation 2 can be written

as

$$\overline{r^2} = 4 \int_0^t \overline{v'^2(t')} dt' \int_0^{t'} e^{-\alpha\tau} \sqrt{\overline{v'^2(t' - \tau)}} d\tau \quad (10)$$

Since α is large, $e^{-\alpha\tau}$ approaches zero very rapidly as τ increases,

so $\sqrt{\overline{v'^2(t' - \tau)}}$ can be approximated by $\sqrt{\overline{v'^2(t')}}$ in the integration.

Thus the equation becomes

$$\begin{aligned} \overline{r^2} &\approx 4 \int_0^t \overline{v'^2(t')} dt' \int_0^{t'} e^{-\alpha\tau} d\tau \\ &= 4 \int_0^t \overline{v'^2(t')} \left[\frac{1}{\alpha} - \frac{1}{\alpha} e^{-\alpha t'} \right] dt' \end{aligned}$$

The second term in the bracket is much smaller than the first and can be neglected. The resulting equation is

$$\overline{r^2} \approx \frac{4}{\alpha} \int_0^t \overline{v'^2}(t') dt'$$

Changing the integration variable from t to z , and taking \bar{u} to be constant for the range of integration (see Figure 4), the result is

$$\overline{r^2} \approx \frac{4}{\alpha \bar{u}} \int_{z_I}^z \overline{v'^2}(z) dz \quad (11)$$

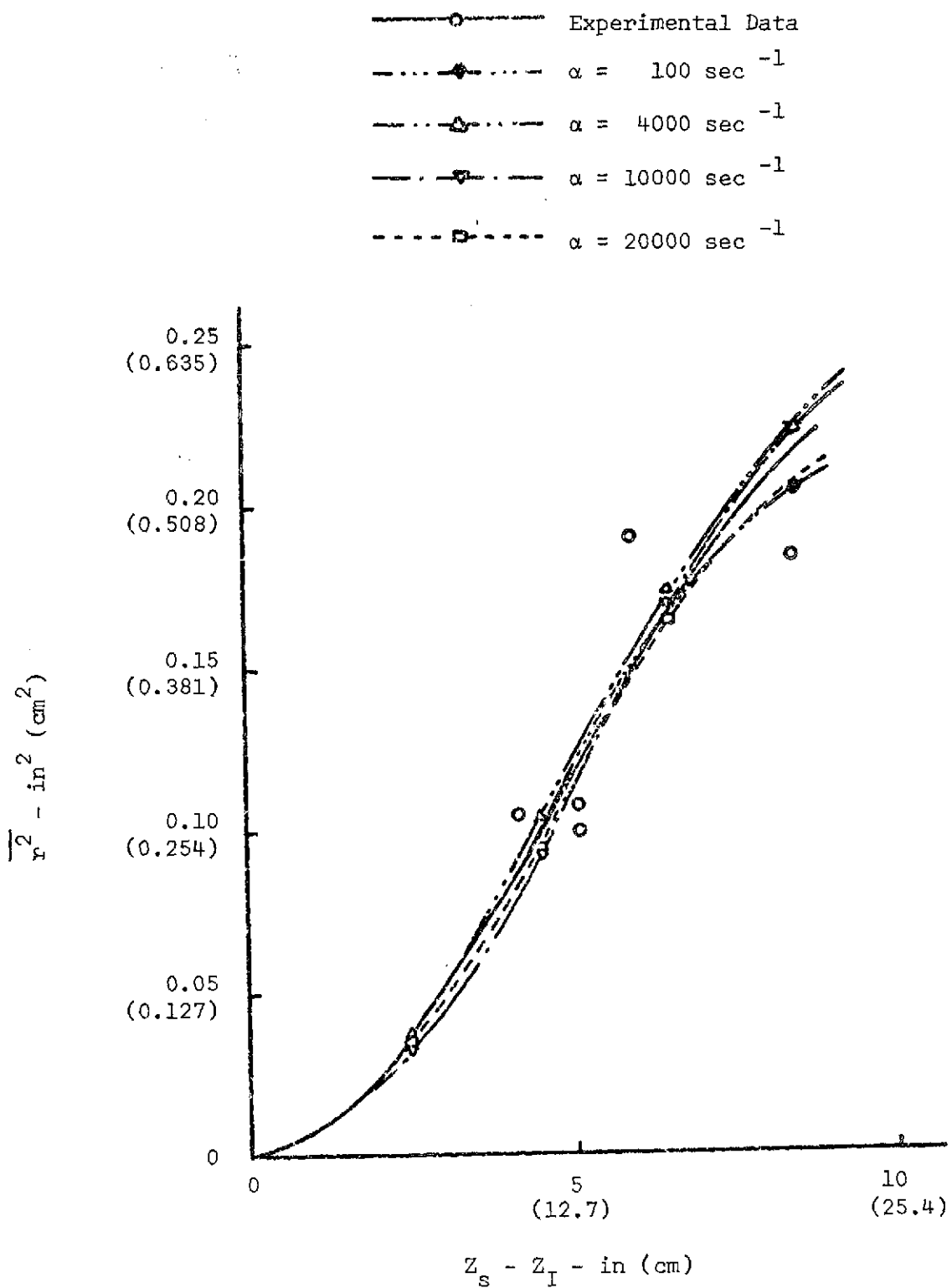
From this equation, it is clear that, for a fixed value of $\overline{r^2}$, $\overline{v'^2}$ increases as α increases as long as α is large.

For an isotropic turbulence field, the intensity of turbulence is defined as

$$T = \frac{\sqrt{\overline{v'^2}}}{\bar{u}} \quad (12)$$

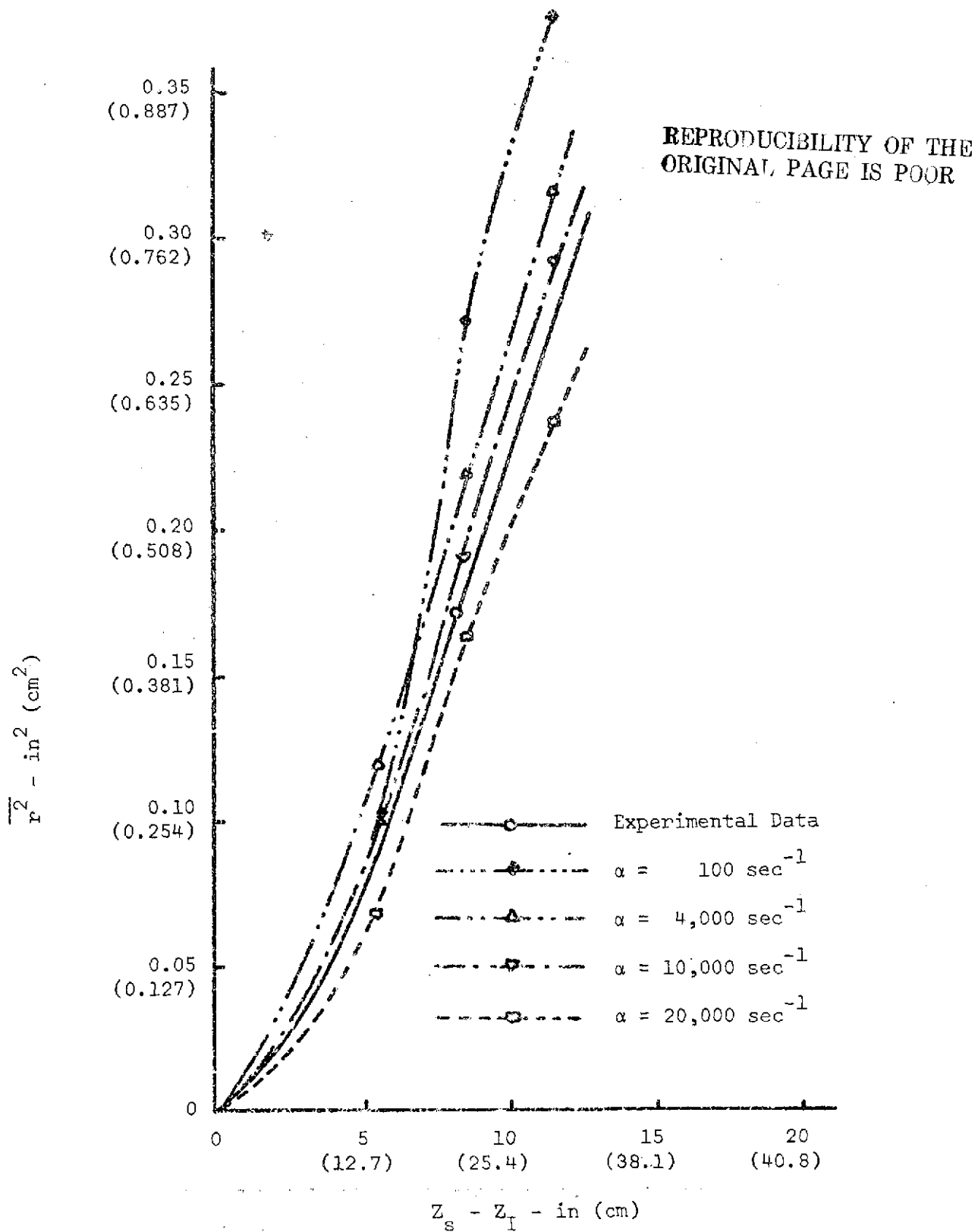
The intensities of turbulence for the three large values of α were calculated. They are shown in Figure 7. The results indicate that, for $\alpha = 10000 \text{ sec}^{-1}$, the intensity of turbulence reaches a maximum value of about 15% near the propellant injector, and decreases to about 4% near the nozzle.

In addition to the results of the present work, the results of the intensity of turbulence obtained by O'Hara et al. (Reference 3) for their liquid rocket combustion chamber are also plotted in Figure 7. The comparison of these results shows that the intensity of turbulence for the liquid rocket combustion chamber is higher than that for the gaseous rocket combustion chamber. It is noted that, besides the differences in the propellants and the types of injectors used, the two rocket combustion chambers are similar.



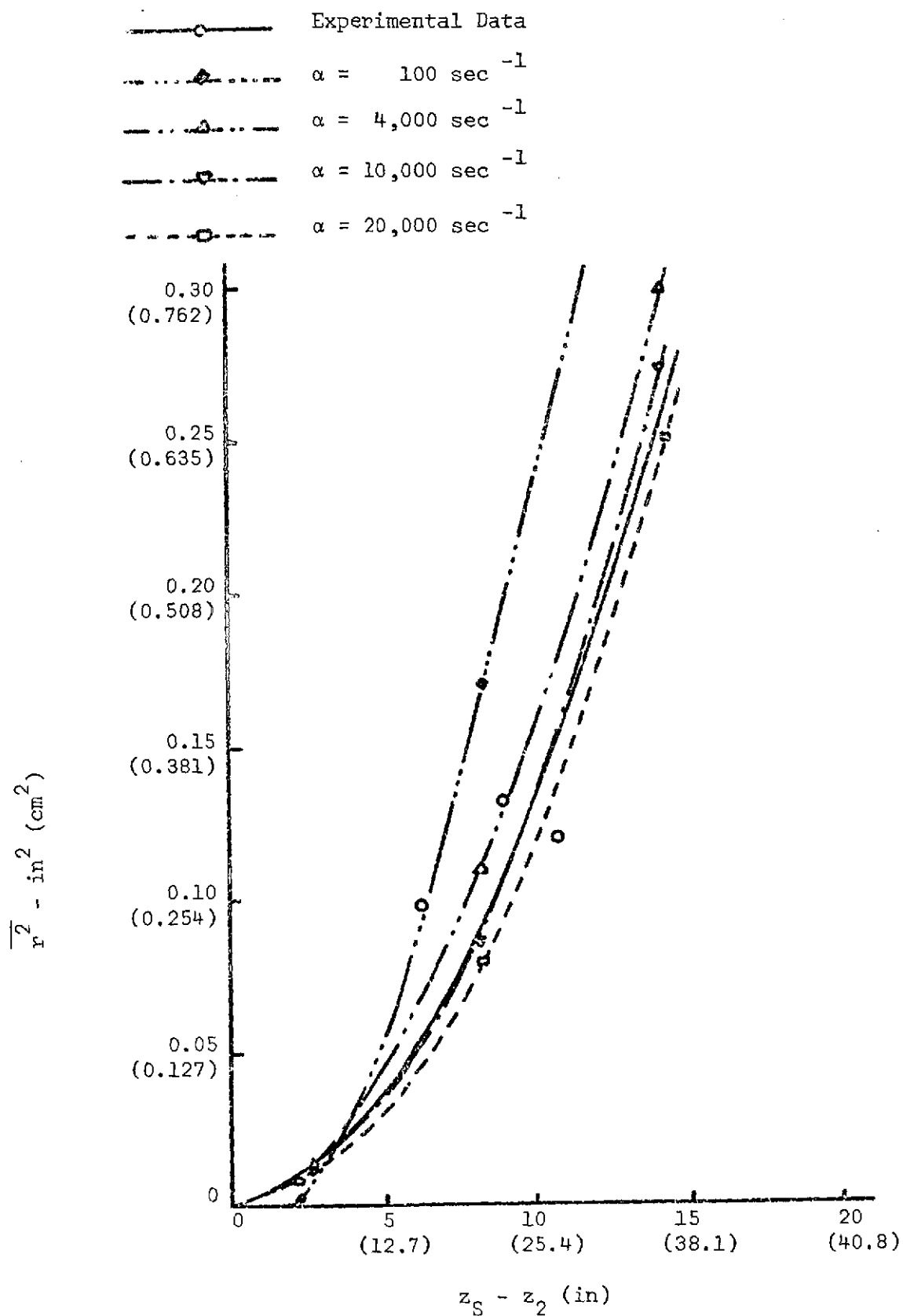
(a) $Z_s = 8.53 \text{ in (21.67 cm)}$

Figure 5. Comparison of Experimental and Calculated Mean Square Dispersion Radii



(b) $Z_s = 11.54 \text{ in (29.31 cm)}$

Figure 5 Comparison of Experimental and Calculated Mean Square Dispersion Radius



(c) $z_S = 14.3 \text{ in (36.32 cm)}$.

Figure 5 Comparison of Experimental and Calculated Mean Square Dispersion Radius

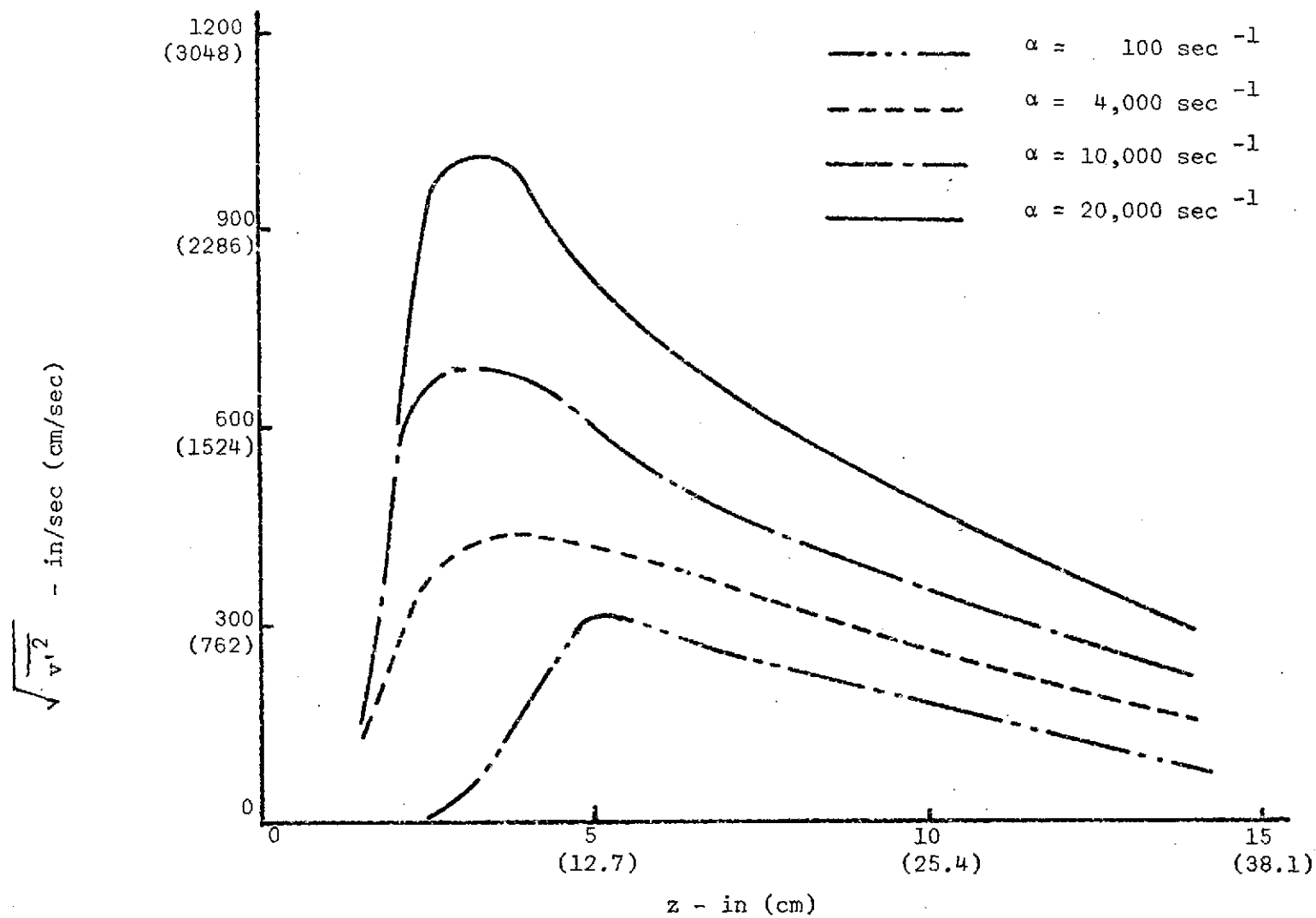


Figure 6 Root Mean Square
Turbulent Velocity

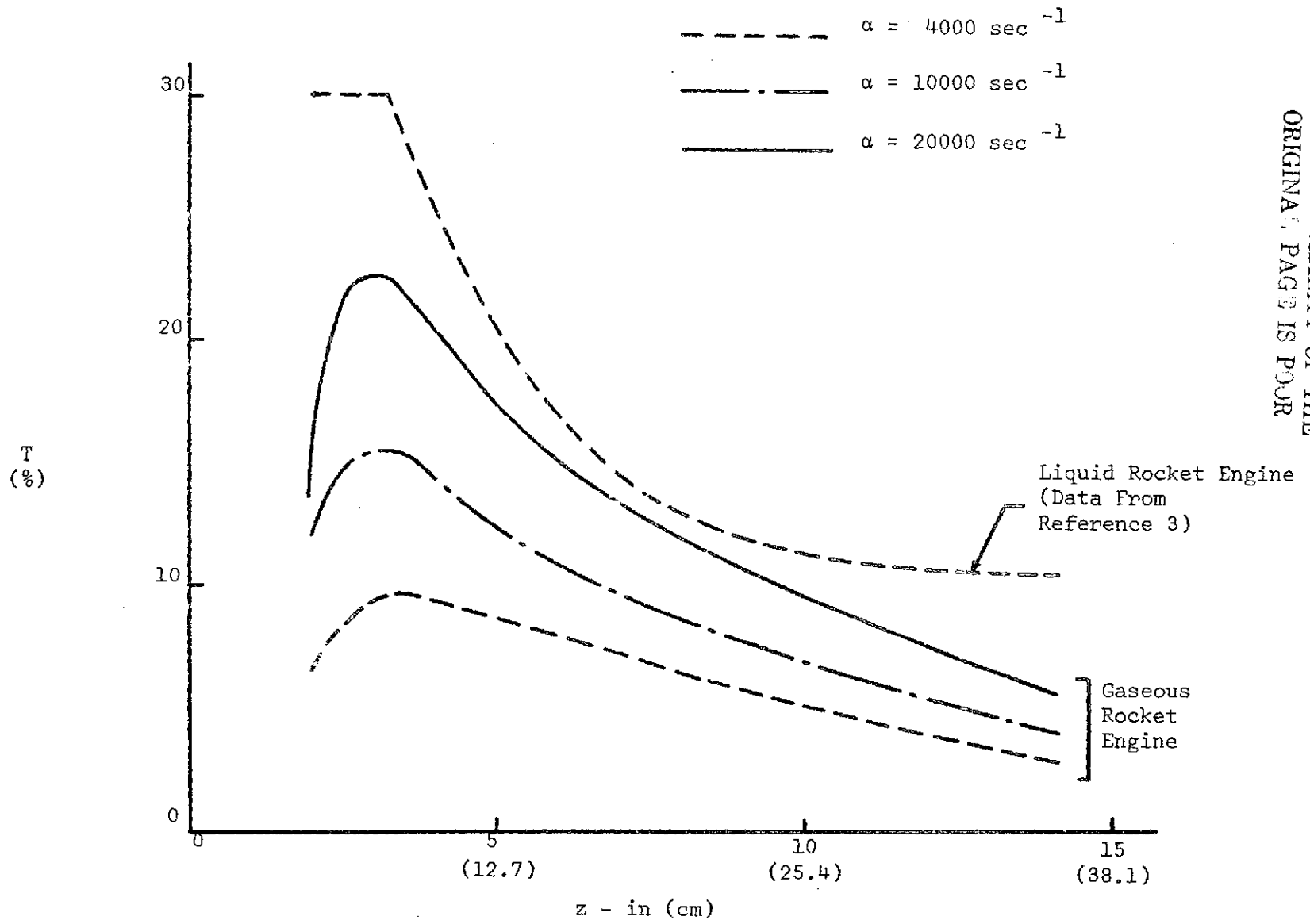


Figure 7 The Intensity of Turbulence

IV. ANALYTICAL DETERMINATION OF THE HELIUM CONCENTRATION

(1) Preliminary Remarks

The distribution of the helium concentration in the combustion chamber was also calculated analytically, in addition to that measured in the experiment. The purpose of this calculation is to check the validity of the effective viscosity formula (Equation 8).

In the theory of turbulent flow (see Reference 7), it has been shown that the mean square dispersion radius is related to the effective diffusion coefficient by the expression

$$D_{\text{eff}} = \frac{1}{4} \frac{dr^2}{dt} \quad (13)$$

In turn, the effective diffusion coefficient is related to the effective viscosity through the Schmidt number which is defined as

$$Sc = \frac{\mu_{\text{eff}}}{\rho D_{\text{eff}}} \quad (14)$$

For the gas mixture dealt with in the present work, the Schmidt number is approximately equal to unity. Therefore, if, at the same helium injection point and sampling station, the mean square dispersion radius obtained from the experiment agrees with that obtained from the calculation, then the effective viscosity formula will be valid for the flow field.

(2) Governing Equations

For determining the helium concentration, the equation of the conservation of helium is needed, in addition to the three equations for determining the flow field as discussed in Part 2 of Section III.

Since helium is an inert gas, the source term in the equation of conservation of helium is zero. Let m_{He} denote the helium concentration. Then the equation of the conservation of helium can be written as

$$\begin{aligned} \frac{\partial}{\partial z} (m_{He} \frac{\partial \psi}{\partial r}) - \frac{\partial}{\partial r} (m_{He} \frac{\partial \psi}{\partial z}) - \frac{\partial}{\partial z} (\rho D_{He,eff} r \frac{\partial m_{He}}{\partial z}) \\ - \frac{\partial}{\partial r} (\rho D_{He,eff} r \frac{\partial m_{He}}{\partial r}) = 0 \end{aligned} \quad (15)$$

If the Schmidt number is assumed to be unity, then $\rho D_{He,eff} = u_{eff}$.

Thus Equation 15 becomes

$$\begin{aligned} \frac{\partial}{\partial z} (m_{He} \frac{\partial \psi}{\partial r}) - \frac{\partial}{\partial r} (m_{He} \frac{\partial \psi}{\partial z}) - \frac{\partial}{\partial z} (u_{eff} r \frac{\partial m_{He}}{\partial z}) \\ - \frac{\partial}{\partial r} (u_{eff} r \frac{\partial m_{He}}{\partial r}) = 0 \end{aligned} \quad (16)$$

It is noted that this equation is in the standard form (Equation 7).

(3) Boundary Conditions

For determining the helium concentration, it is necessary to consider the flow field in the combustion chamber with seven propellant injector elements. This flow field may be approximated using the results obtained for predicting the flow field of one injector element as discussed in the preceding section. The method of approximation will be discussed later.

Since the equation of the conservation of helium is of the elliptic type, boundary conditions are to be specified at every point of the closed boundary surrounding the field of interest. Figure 8 shows the boundary conditions.

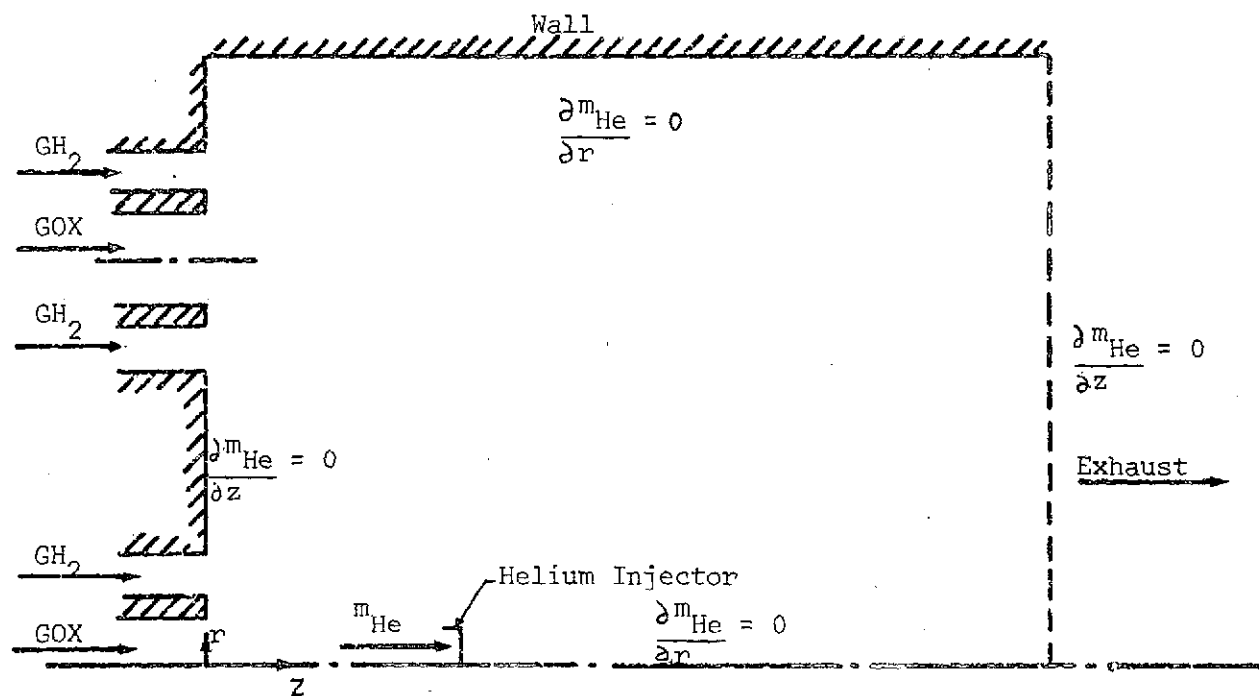


Figure 8 The Boundary Conditions For Determining The Helium Concentration

At the exhaust end there should be no change in the helium concentration. The boundary condition at the exhaust end is $\frac{\partial m_{\text{He}}}{\partial z} = 0$

Along the axis of symmetry or a wall, there should be no helium crossing these boundaries. Therefore the boundary conditions are $\frac{\partial m_{\text{He}}}{\partial z} = 0$ for a vertical boundary ($z = \text{constant}$), and $\frac{\partial m_{\text{He}}}{\partial r} = 0$ for a horizontal boundary ($r = \text{constant}$).

To compute the helium concentration at the helium injection outlet, it is assumed that the pressure, temperature and velocity of helium are the same as those of the flow field at that location. Thus the helium flow rate \dot{m}_{He} is given by

$$\dot{m}_{\text{He}} = \rho_{\text{He}} A_I V_z \quad (17)$$

With the helium density known from this equation, the helium concentration at the helium injector outlet is calculated by

$$m_{\text{He}} = \frac{\rho_{\text{He}}}{\rho + \rho_{\text{He}}} \quad (18)$$

where ρ is the density of the flow field.

(4) Calculation Procedure and Results

Spalding's numerical method was used to solve the governing equations. A computer program based on this numerical method was developed. The details of this computer program were presented in Reference 8.

As discussed earlier in this Section, there were four differential equations to be solved. However, three of these equations were concerned with the flow field and were solved for determining the mean axial flow velocity. Therefore, it was only necessary to use the flow field data available to solve the equation of the conservation of helium.

This was possible, because it was assumed that the small amount of helium flow does not significantly alter the existing flow field.

There were two cases of the helium concentration calculated:

(a) The helium concentration for sampling on the outer propellant injectors ($\theta = 105^\circ$ in Figure 1); and (b) The helium concentration for sampling between the outer propellant injectors ($\theta = 135^\circ$). In approximating the flow field in the combustion chamber for the case of sampling on the outer injectors, the flow field data of the outer injectors were duplications of those of the center injector. But, for the case of sampling between the outer injectors, the flow field values in the regions between the two outer injectors were assumed to be constant and were set equal to the values on the enclosure of the center injector.

The comparison of the experimental and calculated helium concentration profiles is shown in Figure 9. The curves and data points in this figure were normalized, i.e., each value of the helium concentration was divided by the value of the helium concentration at $r = 0$. The normalization was necessary because the magnitude of the helium concentration obtained from the experiment was different from that obtained from the calculation at a corresponding location. Further, in comparing the results, only the shapes of the helium concentration profiles are important.

As can be seen in Figure 9, the shapes of the helium concentration profiles obtained from the experiment and those from the calculations are in good agreement. This indicates that the effective viscosity formula (Equation 8) with $k = 0.012$ is satisfactory for the present work.

Helium Concentration

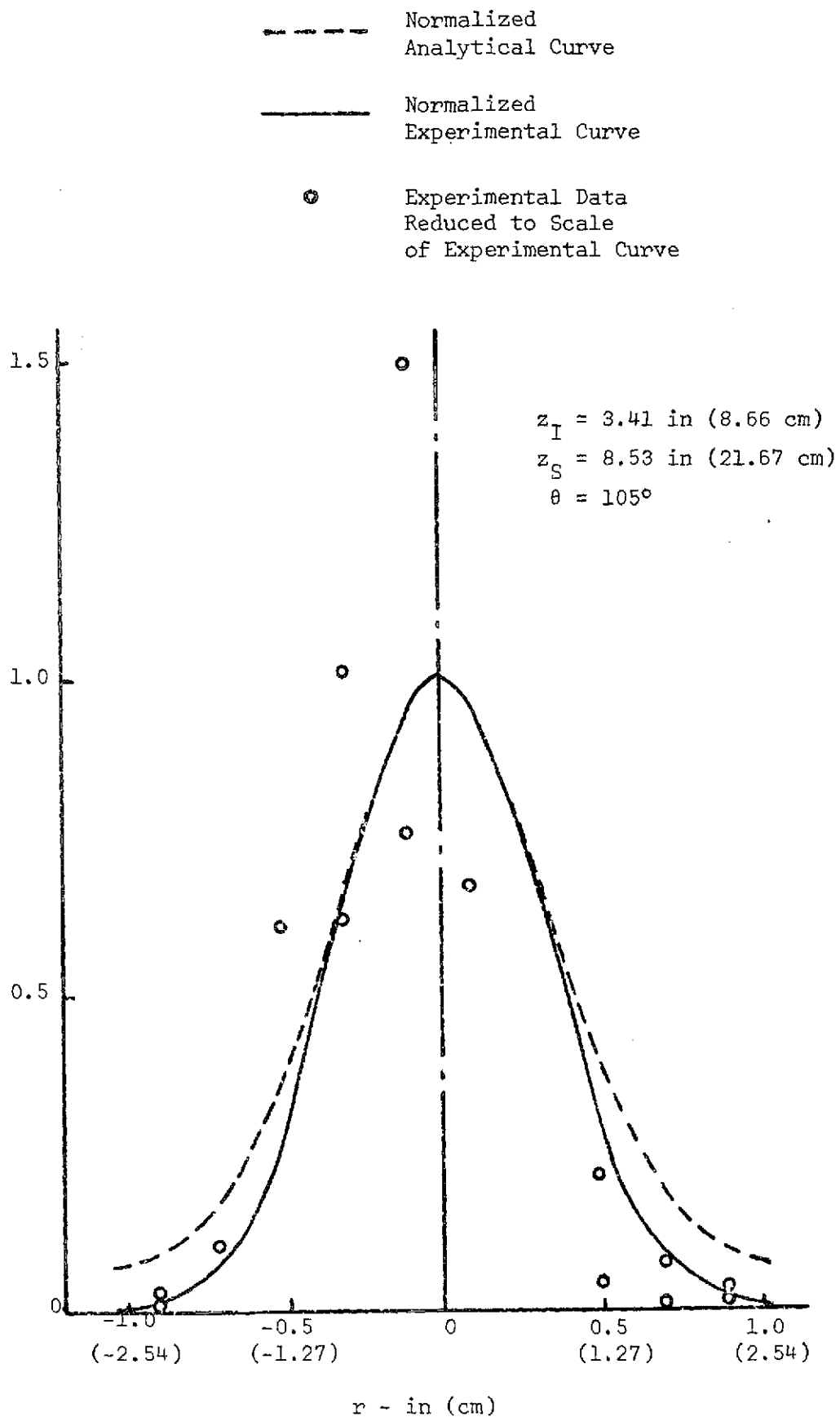


Figure 9a, Comparison of Calculated and Experimental Helium Concentration Profiles

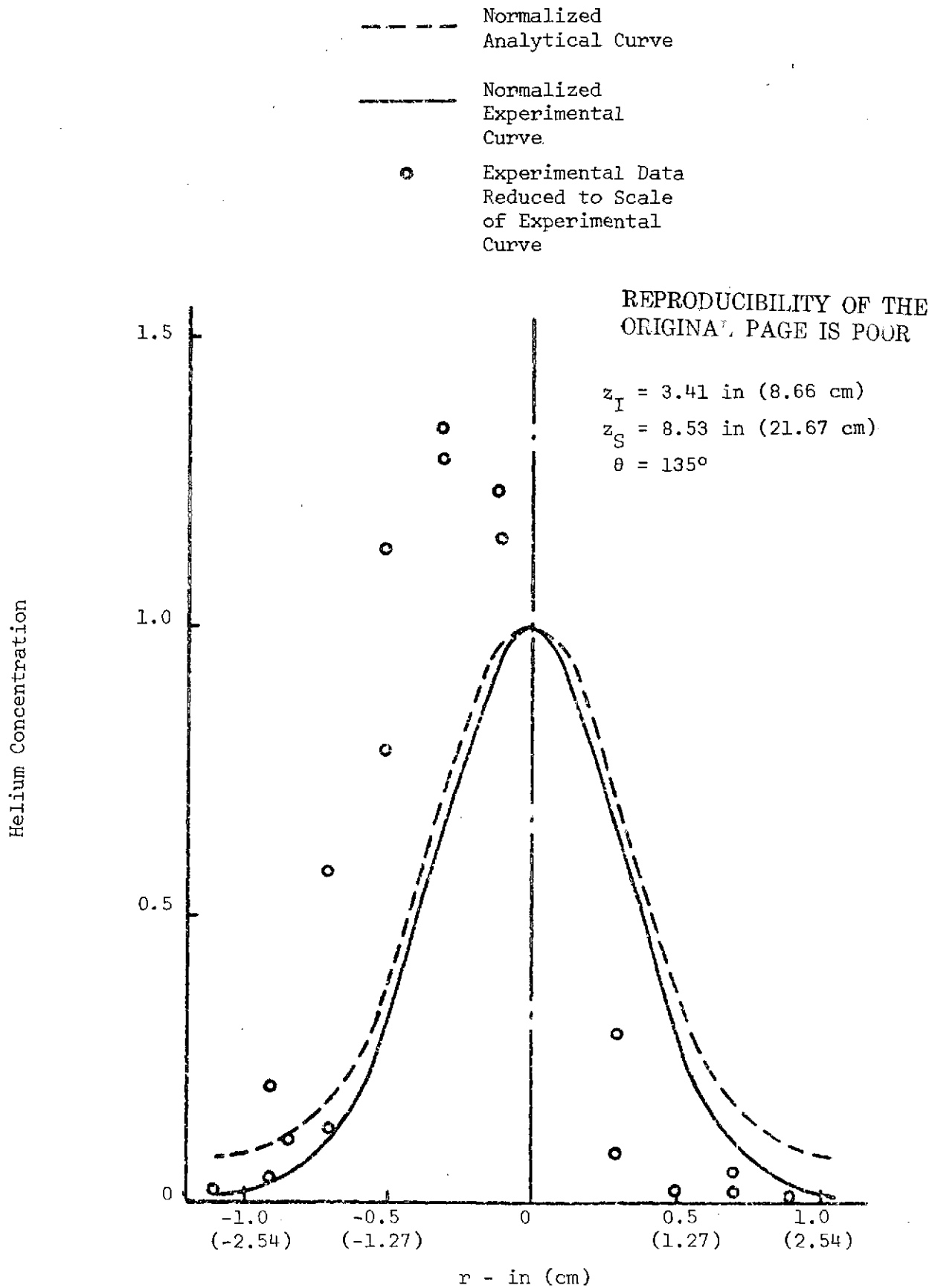


Figure 9b, Comparison of Calculated and Experimental Helium Concentration Profiles

Helium Concentration

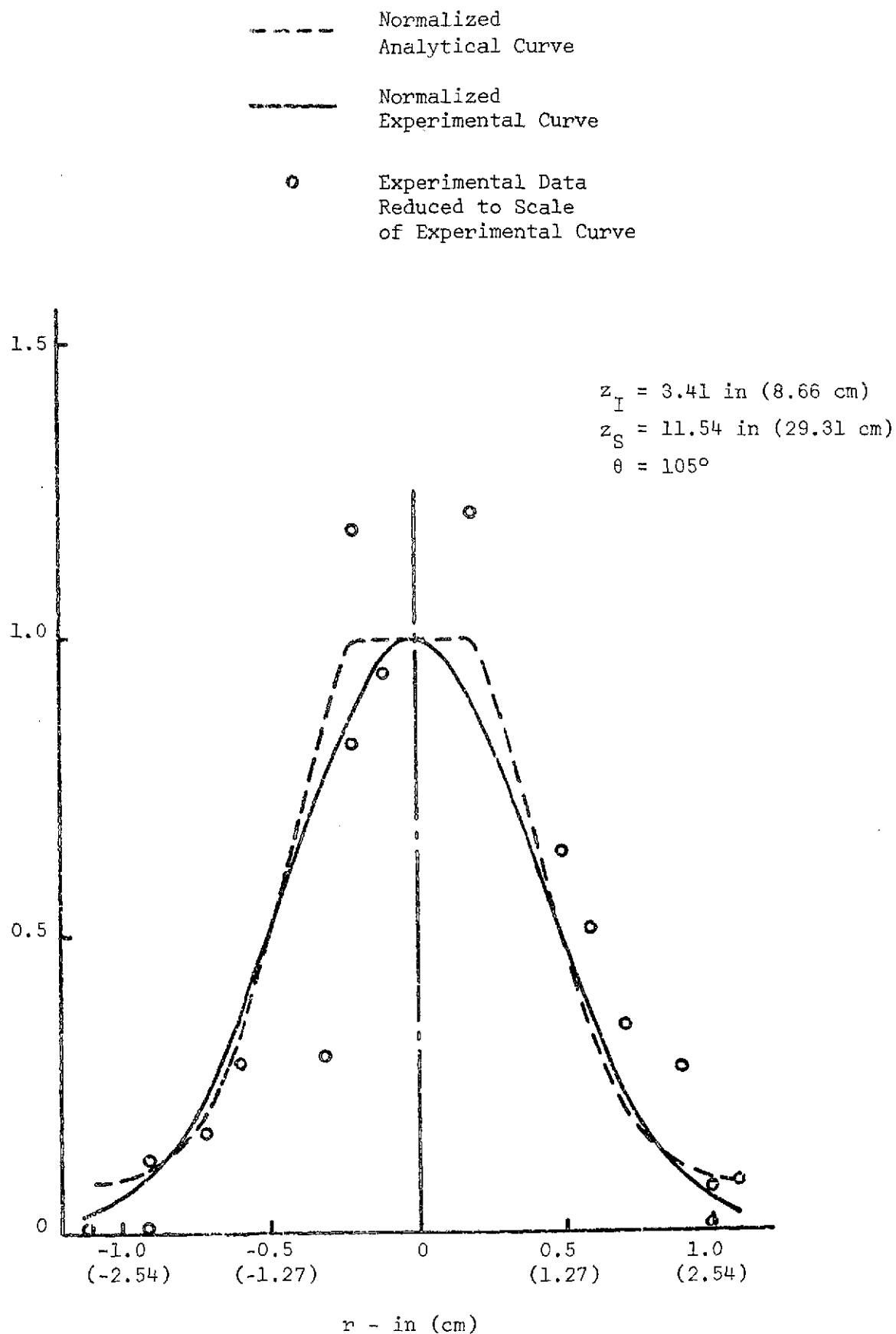


Figure 9c, Comparison of Calculated and Experimental Helium Concentration Profiles

- - - - - Normalized
Analytical Curve
 ————— Normalized
Experimental Curve
 ○ Experimental Data
Normalized to Scale
of Experimental Curve

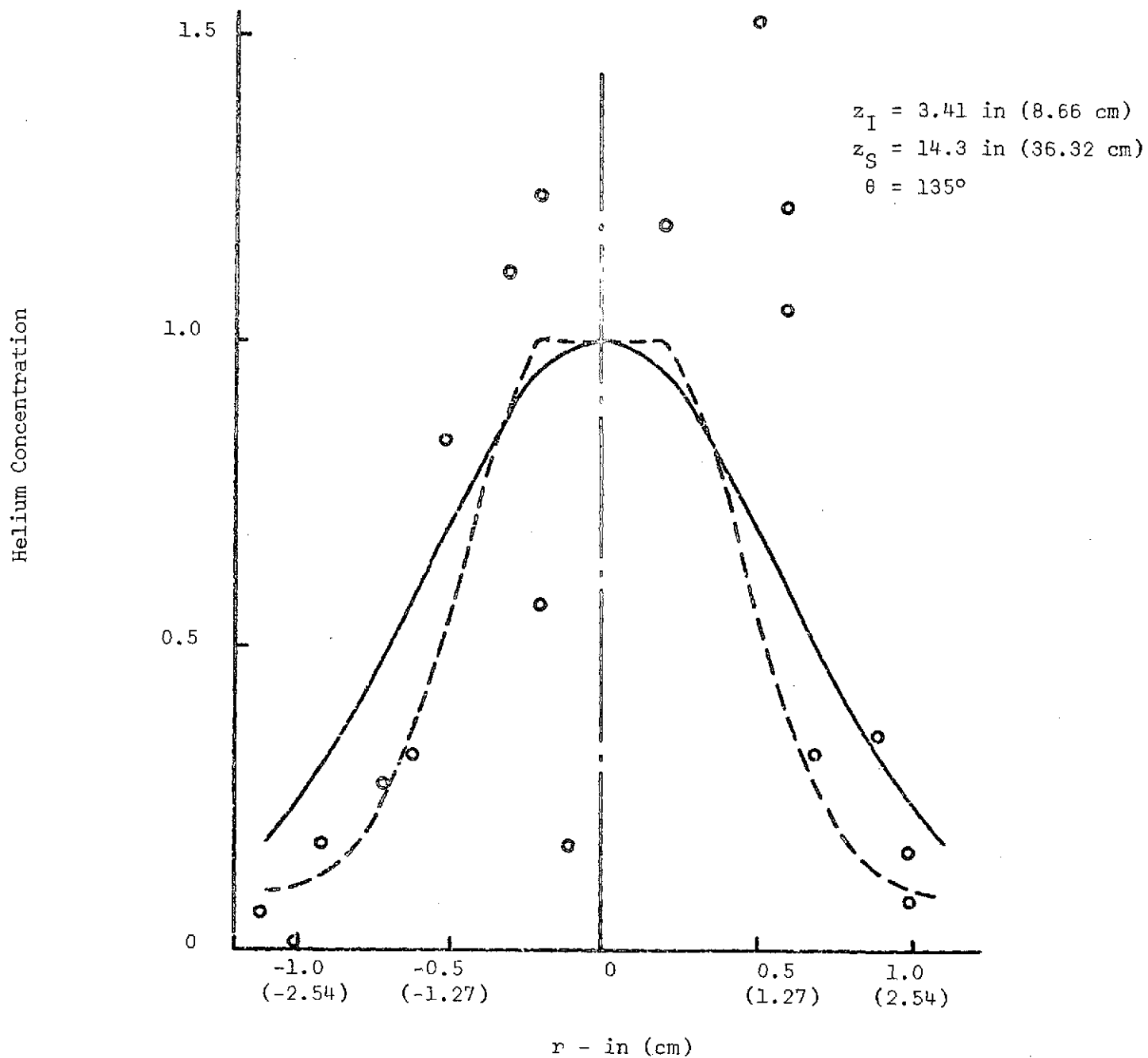


Figure 9d, Comparison of Calculated and Experimental Helium Concentration Profiles

V. CONCLUSION

From the results of the present work, the following conclusions can be drawn:

- (1) For the present rocket combustion chamber, it is satisfactory to assume that the turbulence field is circumferentially homogeneous.
- (2) The turbulent diffusion process in the rocket combustion chamber can be adequately modeled by the one-dimensional Taylor theory.
- (3) The values of the intensity of turbulence vary from a maximum of approximately 15% near the injector to approximately 4% at the nozzle entrance. The Lagrangian correlation coefficient can be represented by the expression $e^{-\alpha t}$ with $\alpha = 10000 \text{ sec}^{-1}$.
- (4) For the turbulent flow in the present rocket combustion chamber, Taylor's turbulent diffusion equation can be reduced to the simple

form

$$\overline{r^2} = \frac{4}{\alpha \bar{u}} \int_{z_I}^z \overline{v'^2}(z) dz$$

- (5) The intensity of turbulence for the liquid rocket combustion chamber is higher than that for the gaseous rocket combustion chamber. The value of the constant α is 4000 sec^{-1} for the liquid rocket combustion chamber and 10000 sec^{-1} for the gaseous rocket combustion chamber.
- (6) The effective viscosity of the flow in the combustion chamber is satisfactorily modeled by the formula:

$$\mu_{\text{eff}} = k d^{2/3} l^{-1/3} \rho^{2/3} (\dot{m}_F V_F^2 + \dot{m}_O V_O^2)^{1/2}$$

with $k = 0.012$.

REFERENCES

- (1) Hersch, M., "Experimental Method of Measuring Intensity of Turbulence in a Rocket Chamber", American Rocket Society Journal, January, 1961, pp. 39-45.
- (2) Bittker, D. A., "An Analytical Study of Turbulent and Molecular Mixing in Rocket Chambers", NACA TN 4321, 1958.
- (3) O'Hara, J., L.O. Smith, and F.P. Partus, "Experimental Determination of the Turbulence in a Liquid Rocket Combustion Chamber", NASA CR-120997, 1972.
- (4) Taylor, G.I., "Diffusion by Continuous Movement", Proc. London Math. Soc., Sec. A, Vol. 20, 1921, pp. 196-212.
- (5) Gosman, A.D., W.M. Pun, A.K. Runchel, D.B. Spalding and M. Wolfshtein, Heat and Mass Transfer in Recirculating Flows, Academic Press, New York, 1969.
- (6) Villalobos, R. and G.R. Nuss, "Measurements of Hydrogen in Process Streams by Gas Chromatography", I.S.A. Transaction, Vol. 4, No. 3, July 1965, pp. 281-286.
- (7) Hinze, J.O., Turbulence, McGraw-Hill, New York, 1959, p. 52.
- (8) Tou, P.P., "An Investigation of the Intensity of Turbulence in a Gaseous Rocket Combustion Chamber", Ph.D. Dissertation, Tulane University, 1974.